J Radioanal Nucl Chem (2011) 288:927–936
DOI 10.1007/s10967-011-1032-z

The effects of physico-chemical properties on natural radioactivity levels, associated dose rate and evaluation of radiation hazard in the soil of Taiwan using statistical analysis

Tsuey-Lin Tsai · Chi-Chang Liu · Chun-Yu Chuang · Hwa-Jou Wei · Lee-Chung Men

Received: 6 February 2011 / Published online: 24 February 2011

Abstract Activity concentrations using gamma-ray spectrometer and distributions of natural radionuclides in soil samples collected were investigated to assess the environmental radioactivity and characterization of radiological hazard. The average concentrations of ^{238}U, ^{232}Th series and ^{40}K in the 5 cm depth soil were 22.53, 33.43 and 406.62 Bq kg^{-1}, respectively, which was within world median ranges in the UNSCEAR 2000 report. The average absorbed dose rate estimated by soil activity and annual effective doses were 49.32 nGy h^{-1} and 60.48 μSv, respectively. Since the soil is an important building material, the mean radium equivalent activity (Ra_{eq}), external (H_{ex}) and internal (H_{in}) hazard index using various models given in the literature for the study area were evaluated as 101.72 Bq kg^{-1}, 0.27 and 0.34, respectively, which were below the recommended limits. The effects of pH value, conductivity, true density and textural properties of soil samples on the natural radionuclide levels were also studied. The application of cluster analysis (CA) and principal component analysis (PCA), coupled with Pearson correlation coefficient analysis, were utilized to analyze the data, identify and clarify the effects of physico-chemical properties on natural radioactivity levels. The CA and PCA results showed that the former method yielded three distinctive groups of the soil variables whereas the latter one yielded the number of variables into three factors with 87.5% variance explanation.

Keywords Natural radionuclides · Soil parameters · Dose rate · Radiation hazard · Cluster analysis · Principal component analysis

T.-L. Tsai · H.-J. Wei · L.-C. Men
Chemical Analysis Division, Institute of Nuclear Energy Research, No. 1000, Wenhua Rd., Longtan 32546, Taiwan, R.O.C

C.-C. Liu
Radiation Monitoring Center, AEC, Cherng-Ching Road, Koahsiung 833, Taiwan, R.O.C

C.-Y. Chuang
Department of Biomedical Engineering and Environmental Sciences, National Tsing Hua University, Hsinchu 30013, Taiwan, R.O.C

T.-L. Tsai (✉)
No. 1000, Wenhua Rd., Jiaan Village, Longtan Township, Taoyuan County 32546, Taiwan, R.O.C
e-mail: polly@iner.gov.tw

Introduction

Taiwan, the largest Mediterranean island (with an extension of about 25,000 km^2), exhibits a very wide variety of lithologies, ranging from sedimentary to metamorphic and volcanic rocks. The major geological features of Taiwan can be broadly classified into three major regions divided by longitudinal faults; the central range which forms the backbone ridge of the island, the western piedmont coast with alluvium and the eastern coastal mountain range [1]. The hilly west coastal region is composed of Oligocene to Pleistocene clastic sediments. The rocks are mainly alternations of sandstones and shales with locally interspersed limestone and tuff. The modern alluvium is predominantly made up of clay, silt, sand and gravel, and covers the plain and basin area. The flood plain is composed of alluvium which also occupies the floor of the river valleys and coastal sand and sand dunes. The eastern part of the island, starting from the central mountain range toward the Pacific Ocean, is composed of metamorphic rock of the earlier Mesozoic and Paleozoic eras. Other areas, like Tatun Shan

located in the north, the eastern coastal mountain range and many outlying islets, such as Penghu archipelago, are comprised of lava flow, agglomerates-masses of volcanic rock fragments fused by andesite and basalt [2]. The geological map of Taiwan and studied area were shown in Fig. 1.

The terrestrial component of the natural background is dependent on the compositions of soils, rocks and some building materials, which typically contain natural radionuclides. Determination of soil radioactivity is essential to understanding changes in the natural radiation background. Gamma radiation emitted from environmental natural radioactivity levels results in terrestrial background radiation, which varies the geological and geographical structure and dominates external radiation dose to human body [3]. Under normal circumstances, the artificial radioactivity emitted from the nuclear power plants, industrial plants and research facilities has smaller contribution to the overall radiation. Soil generally contains small quantities of radioactive elements, U and Th along with their progeny and the primordial radionuclides of external radiation are ^{238}U, ^{232}Th series and ^{40}K. Although the ^{235}U series also exists in soil, it accounts for a very small contribution to human body. Soil may have been produced from the weathered top layer of still-intact bedrock below or transported laterally from the same rock unit. Variation of background concentrations of radionuclides in soil depends on the type, moisture content, inhomogeneity of its permeability, formation, transport processes and geomorphology [4] associated with meteorological conditions. Soil formation and chemical and biochemical interactions also influence the distribution patterns of U, Th and their decay products [5]. Radioactivity in soil results from the rock from which it is derived, including decrease by leaching of water, dilution by increased porosity and by added water and organic matter, and increase by sorption and precipitation of radionuclides from incoming water [6].

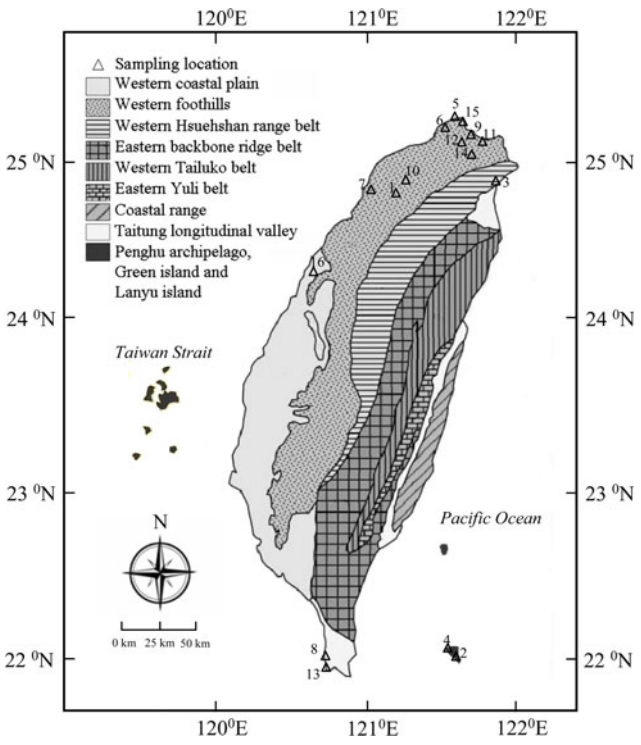

Fig. 1 Geological map showing sampling locations in Taiwan

The univariate statistics normally used are too limited for this objective, while a multivariate analysis takes into account many variables analyzed simultaneously to give much more information about the characteristics of a soil. Therefore, the consideration of several properties and multivariate analytical methods will be necessary for a greater understanding of soil processes.

The radioactivity concentrations and dose assessment for soil samples around specific area in Taiwan have been previously investigated [7], however, the effects of physico-chemical properties on naturally occurring radionuclides in the soil have not been studied yet. The objective of this work was to establish baseline statistical information of background levels of naturally occurring radionuclides due to ^{238}U, ^{232}Th series and ^{40}K present in the soil and their relationship to physico-chemical properties of soil. The radium equivalent activity associated health hazards, gamma- absorbed dose rate in air based on activity concentrations of natural radionuclides and annual effective dose rates had also been estimated and also compared with different countries of the world. Besides, the homogenous groups and the groups responsible for explaining the combined variances and making the significant differences using the multivariate statistical methods were identified and interpreted.

Experimental

Sample collection and preparation for radionuclide analysis

Soil samples were collected from 16 different locations, covering some area of currently commercial near-by nuclear power plants, Lan-Yu temporary storage site for low-level radwaste and around nuclear facility. Topsoil samples at a depth of 5 cm, collected from 9 sub-samples at interline distance of 5 m from a 10 × 10 m^2 rectangular grid of entire area for each site, were mixed together to obtain a representative sample. Undisturbed sampling sites were chosen to ensure that samples were representative of the areas. Grass and pieces of wood were manually eliminated from the samples which were stored in stainless steel containers until analysis. The samples were dried at 105 °C

for 24 h to remove moisture, then subsequently crushed, ground to fine powder, homogenized by passing through a 2 mm test sieve, weighed and stored in an air-tight plastic jar of 125 mL at room temperature for 1 month before gamma counting. Samples were firmly sealed to allow the attainment of all daughters in equilibrium with their parents in the decay chain and the effect of radon emanation was not taken into account.

Soil parameters

In the soil samples, the following physico-chemical parameters were measured by conventional methods. For the size distribution, percentages of clay, silt, and sand in the soil samples were performed by mechanical shaking of sieves. Soils were divided into three fractions: coarse sand (0.2–2 mm); fine sand (0.002–0.2 mm); (clay + silt) <0.002 mm. Each fraction was weighed and its percent weight was also calculated. The pH values were determined with a glass electrode in an aqueous suspension of 10 g of dry soil and 25 mL of distilled water, stirred and left to stand overnight. True densities of soil were determined using an Ultrapycnometer 1000 (Quanta Chrome) with PYCWIN software (v.2). The conductivity in soil was measured in a water extract, after shaking 20 g of air-dried soil with 100 mL of distilled water for 1 h. Data were corrected to 25 °C.

Instrumentation, calibration and radioactivity measurements by gamma spectrometry

A gamma spectrometer and relevant accessories were supplied by Canberra, USA. Each sample was analyzed using a high-purity germanium (HPGe) detector, connected to the following components: preamplifier, amplifier, ADC converter and acquisition interface module (AIM, model 556B). Qualitative and quantitative analysis of gamma spectra were processed using the GENIE 2000 program. The detector was surrounded by a special heavy-lead shield about 10 cm thick with inside dimensions of 28 cm in diameter × 40.5 cm in height. The shield was utilized to minimize background radiation. Characteristic X-rays from lead was reduced using a 1.2 cm thick layer of copper. Detector output was connected to an FT Research Amplifier (Model 2025). The full width at half maximum (FWHM) is 1.9 keV for the 1332.5 keV gamma-ray line of ^{60}Co. The efficiency of the detector is approximately 40% relative to 3 × 3 in^2. NaI(Tl). Energy calibration and efficiency calibration of the spectrometer to maintain measurement quality were carried out using a standard mixed multi-nuclide source, traceable to the US National Institute of Standard and Technology (NIST) standard. The calibration sources contained ^{241}Am, ^{109}Cd, ^{57}Co, ^{139}Ce, ^{203}Hg, ^{113}Sn, ^{85}Sr, ^{137}Cs, ^{88}Y and ^{60}Co peaks for the energy range of 88–1836 keV. The standards and samples were prepared with a uniform geometry. All the samples and background were counted for a period of 80,000 s in order to get sufficient counts at the desired peaks.

The activity concentrations of ^{238}U and ^{232}Th were calculated assuming a secular equilibrium with their decay products. The activity concentration of ^{238}U was determined through photopeaks of its daughters ^{214}Pb (295.2 and 351.9 keV) and ^{214}Bi (609.3 and 1120.3 keV), while the activity concentrations of ^{228}Ac (911.1 and 969.1 keV), ^{208}Tl (583.1 and 860.6 keV), ^{212}Pb (238.6 keV) and ^{212}Bi (727.2 keV) were assumed to represent ^{232}Th activity [8]. The ^{238}U and ^{232}Th activities were derived using an average value of their progenies. The activity concentration of ^{40}K was measured directly from its 1460.8 keV gamma-ray peak. Activity levels of samples obtained for ^{214}Pb, ^{214}Bi, ^{228}Ac, ^{208}Tl, ^{212}Pb, ^{212}Bi and ^{40}K are expressed in Bq kg^{-1}.

Statistical treatment

Conventional and multivariate statistical procedures for data treatment and graphics were performed using the commercial statistics software package SPSS version 12.0 for Windows.

Cluster analysis and Pearson correlation were carried out in order to clarify the relationship among the variables, especially the influence of soil parameters on the distribution of natural radionuclides. Cluster analysis is a useful statistical method which presents visually the degree of association among variables. The distance axis displays the degree of association between groups of variables, i.e., the lower the value on the axis, the more significant the correlation [9].

Principal components analysis (PCA) is the most common technique used to summarize patterns among variables in multivariate datasets. The PCA is a way of identifying patterns in variables, and expressing data in such a way as to highlight their similarities and differences. The main advantage of PCA is that, once the patterns have been found, data can be compressed reducing the number of dimensions, without much loss of information.

Results and discussion

Distribution of natural radioactivity in soil samples

Table 1 presented the activity concentrations of the ^{238}U, ^{232}Th series and ^{40}K in the samples. The ± values of radioactivity concentrations represented the counting

Table 1 Activity concentrations of the ^{238}U, ^{232}Th series and ^{40}K (Bq kg^{-1}), radium equivalent activity (Ra_{eq} in Bq kg^{-1}), external and internal hazard indices (H_{ex}; H_{in}), representative level index ($I_{\gamma r}$ in Bq kg^{-1}), calculated absorbed dose rate in air from terrestrial gamma radiation (D in nGy h^{-1}) and annual effective dose (AED in μSv a^{-1}) of studied samples

Sample code	^{238}U series	^{232}Th series	^{40}K	Ra_{eq}	H_{ex}	H_{in}	D	AED
1	17.98 ± 1.56	28.92 ± 3.75	383.10 ± 24.67	88.81	0.24	0.29	43.37	53.19
2	34.79 ± 2.57	50.89 ± 5.44	297.70 ± 22.30	130.4	0.35	0.45	61.41	75.31
3	27.96 ± 1.78	45.57 ± 5.26	598.46 ± 32.54	139.16	0.38	0.45	67.96	83.35
4	9.17 ± 1.46	11.20 ± 4.06	255.65 ± 20.66	44.86	0.12	0.15	22.37	27.44
5	33.80 ± 2.91	53.77 ± 7.35	505.69 ± 40.14	149.56	0.40	0.50	71.87	88.14
6	46.15 ± 2.65	65.55 ± 7.03	390.68 ± 31.23	169.90	0.46	0.58	79.98	98.08
7	30.63 ± 2.12	43.61 ± 6.49	558.38 ± 36.16	135.94	0.37	0.45	66.07	81.03
8	21.08 ± 1.72	25.84 ± 4.12	268.31 ± 21.73	78.65	0.21	0.27	37.69	46.23
9	32.55 ± 2.79	63.11 ± 7.44	627.42 ± 42.93	171.05	0.46	0.55	82.78	101.52
10	29.91 ± 2.40	49.72 ± 6.27	674.98 ± 37.83	152.93	0.41	0.49	74.84	91.79
11	12.65 ± 1.36	13.28 ± 3.46	365.60 ± 23.65	59.78	0.16	0.20	29.99	36.78
12	11.94 ± 1.47	13.28 ± 2.76	257.74 ± 16.61	50.76	0.14	0.17	25.02	30.69
13	3.60 ± 0.68	3.96 ± 0.38	73.60 ± 6.12	14.92	0.04	0.05	7.33	9.00
14	10.94 ± 1.47	14.86 ± 4.05	371.56 ± 24.73	60.79	0.16	0.19	30.56	37.48
15	14.11 ± 1.80	20.00 ± 4.52	419.93 ± 31.08	75.02	0.20	0.24	37.40	45.87
16	23.23 ± 1.44	31.40 ± 3.91	457.18 ± 26.50	103.30	0.28	0.34	50.45	61.88
Worldwide median range	16–110	11–64	140–850				18–93	
Median value (UNSCEAR2000)	35	30	400				57	

uncertainty with a coverage factor of $k = 2$. In all sampling sites, mean activity concentration is of the order ^{238}U < ^{232}Th < ^{40}K. As seen in the table, the activity concentration of ^{40}K in soil is an order of magnitude higher than that of ^{238}U and ^{232}Th, which is also in agreement with the well-known fact that potassium in the earth's crust is of the order of percentage while U and Th are in ppm level. In addition, the activity concentration of Th is higher than that of uranium due to the low geochemical mobility and insoluble nature in water of thorium [10]. In other words, uranium is relatively more susceptible to be soluble, whereas thorium is easily adsorbed by soil. The average concentrations of ^{238}U, ^{232}Th series and ^{40}K were 22.23, 33.43 and 406.62 Bq kg^{-1} (dry weight), respectively. The worldwide median values are 35, 30 and 400 Bq kg^{-1} for ^{238}U, ^{232}Th series and ^{40}K, respectively [11]. Hence, the mean activities of these radionuclides in sampling locations were comparable with world median ranges.

Good correlation coeffecient ($R^2 = 0.94$) with linear regression line was obtained between ^{238}U and ^{232}Th in soil samples. Patra et al. [8] and Jabbar et al. [12] also reported that the correlation coefficients between ^{238}U and ^{232}Th activity were 0.90 and 0.91 in soil samples around Kaiga site, India and Islamabad, Pakistan, respectively. However, weak and positive correlation coefficients between ^{238}U and ^{40}K and between ^{232}Th and ^{40}K were 0.36 and 0.48, respectively, which was similar to the results of other literature [13]. It was expected that ^{238}U and ^{232}Th correspond to natural decay series, where as ^{40}K, though naturally occurring radionuclide, but not belongs to part of any such decay series.

The natural radioactivities did not have a uniform distribution depending on radioactivity of rocks forming the geological structure in this region. The sample number code 13, located around nuclear power plant (III) was white sand with the lowest activity concentrations for each of the three natural radionuclides ^{40}K (Table 1). Ibrahim et al. also reported the highest radionuclide activity occurred in clay soils, whereas the lowest occurred in sandy soils in the Nile Delta and middle Egypt [14].

As shown in Table 2, the mean activity concentration of ^{238}U in the soils of studied area was the lowest among the countries [7, 8, 15–21], but comparable with the previous study [7]. Similarly, the value of ^{232}Th was lower than that of many countries like Hong Kong, Japan, Kotagiri of India and Pakistan, but higher than that of Bangladesh, Kaiga of India, Turkey and Venezuela. The measured value of ^{40}K in the present work was higher than those of Hong Kong, India, Turkey and Venezuela, but slightly above the earlier findings [7].

Calculation of radium equivalent activity (Ra_{eq}) and hazard indices

Concentration of natural radioactivity in building materials also reflects the geological variations of the sites of origin. In Taiwan, some buildings are constructed from soil and rock based materials such as sands, gravels, cements,

Table 2 Comparison of gamma-ray activity concentrations in soil samples and dose rates reported from different countries of the world

Location	Mean activity concentration (Bq kg^{-1})			Absorbed dose rate in air (nGy h^{-1})	Reference
	^{238}U	^{232}Th	^{40}K		
Dhaka, Bangladesh	33.0	16.0	574	81.0	[15]
Hong Kong	119	146	352	87.0	[16]
Japan	32.4	54	794	83.0	[17]
Kaiga, India	24.0	31.7	201.4	33.0	[8]
Kotagiri, India	41.4	102.1	229.4	100.1	[18]
Manisa, Turkey	28.5	27	340	54.0	[19]
Mid-Rechna interfluvial region, Pakistan	49.0	62.4	670.6	70.1	[20]
Gung-Liao, Taiwan	24.2	26.4	435.7	46.6	[7]
Taiwan	22.2	33.4	406.6	49.3	This study
Venezuela	27	31	357	–	[21]

bricks and tiles. Among the raw materials, bricks made of soil are the major components of construction materials for conventional villages in suburban area. The radionuclides in soil are a source of external gamma exposure and internal radon exposure. The assessment of building material is based on radium equivalent activity, external and internal hazard indices.

Radium equivalent activity (Ra_{eq})

Radium equivalent activity is a widely used hazard index and is calculated using the following equation [22].

$$\mathrm{Ra_{eq}(Bq\,kg^{-1})} = A_U + 1.429\,A_{Th} + 0.077\,A_K \quad (1)$$

where A_U, A_{Th} and A_K are activity concentrations of ^{238}U ^{232}Th and ^{40}K in Bq kg^{-1}, respectively. Table 1 presented the calculated Ra_{eq} values for the samples collected. The Ra_{eq} values ranged from 14.92 to 171.05 Bq kg^{-1} with an average Ra_{eq} of 101.62 Bq kg^{-1} which was much close to that of other investigation results (104.2 Bq kg^{-1}) reported by Yasir et al. [23] for one of the building materials, soil in Malaysia. The estimated average Ra_{eq} values in this study were lower than the recommended value of 370 Bq kg^{-1} [24].

External hazard index (H_{ex})

The external hazard index H_{ex} was calculated from activity concentrations of the samples using the conservative model proposed by Krieger [25] for limiting the radiation dose from the building materials to 1.5 mGy a^{-1} based on infinitely thick walls without windows and doors as a criterion. The external hazard index is given as

$$H_{ex} = A_U/370 + A_{Th}/259 + A_K/4810 \leq 1 \quad (2)$$

where A_U, A_{Th} and A_K are the activity concentrations of ^{238}U, ^{232}Th and ^{40}K in Bq kg^{-1}, respectively. The value of H_{ex} must be lower than unity in order to keep the radiation hazard insignificant. As shown in Table 1, the H_{ex} values varied from 0.04 to 0.46 with an average of 0.27. The maximum value of H_{ex} is equal to unity, which corresponds to the upper limit of Ra_{eq} (370 Bq kg^{-1}). Since all values are lower than unity, according to the Radiation Protection 112 [26] report, the soil from the studied area is safe and can be used as construction material without posing any significant radiological threat to public health.

Internal hazard index (H_{in})

To address the radiation hazard to respiratory organs posed by radioactive inert gas radon (^{222}Rn), a daughter product of radium and its short-lived secondary products, a second criterion was developed by Krieger [25] to produce the acceptable concentration of radium to half the normal limit, has been used [24]. The hazard index is given as

$$H_{in} = A_U/185 + A_{Th}/259 + A_K/4810 \leq 1 \quad (3)$$

where A_U, A_{Th} and A_K are the activity concentrations of ^{238}U, ^{232}Th and ^{40}K in Bq kg^{-1}, respectively. For the safety of utilizing materials in the construction of buildings, H_{in} should be less than unity. Table 1 displayed H_{in} results based on the criterion given in Eq. 3 and the values ranged from 0.05 to 0.58 with an average of 0.34, which showed that they were less than unity. This index provides a useful guideline in regulating the safety standards on radiation protection for the general public residing in common dwellings.

Calculation of air-absorbed dose rates (D) from soil

The absorbed dose rates (D) were calculated in air from the activity concentrations of ^{238}U, ^{232}Th and ^{40}K concentrations in soil. The conversion factors of gamma-dose rate at 1 m above the soil surface for ^{238}U, ^{232}Th and ^{40}K are 0.427, 0.662 and 0.0432 nGy h^{-1}/Bg kg^{-1}, respectively.

Table 3 The physico-chemical properties of soil in the studied area

Sample code	pH	Conductivity (μs/cm)	True density (g/cm^3)	Coarse sand (%)	Fine sand (%)	Clay + silt (%)
1	7.82	100	2.73	5.23	38.75	56.02
2	5.28	420	2.51	80.02	12.16	7.82
3	7.01	167	2.68	46.13	19.46	34.40
4	5.63	183	2.73	61.73	19.02	19.25
5	3.93	272	2.62	91.41	4.66	3.93
6	4.97	188	2.68	83.22	8.06	8.72
7	4.88	153	2.75	61.72	25.21	13.06
8	7.51	140	2.69	83.81	10.39	5.80
9	4.19	138	2.53	78.87	10.55	10.58
10	4.57	246	2.75	42.16	48.04	9.80
11	7.96	1149	2.71	78.37	21.27	0.36
12	7.81	881	2.88	95.39	3.13	1.48
13	8.23	2510	2.81	99.62	0.26	0.12
14	7.88	626	2.77	46.75	52.53	0.72
15	8.2	2070	2.45	30.74	59.36	9.90
16	7.8	95	2.74	69.55	15.07	15.37
Analytical methods	pH meter	Conductivity meter	Density meter	Mechanical shaking of sieves		

Therefore, the absorbed dose rate (in nGy h^{-1}) in air can be estimated using the following equation [16, 27]:

$$\mathrm{D(nGy\,h^{-1})} = 0.427\,A_{\mathrm{U}} + 0.662\,A_{\mathrm{Th}} + 0.0432\,A_{\mathrm{K}} \quad (4)$$

where A_{U}, A_{Th} and A_{K} are the activity concentrations of ^{238}U, ^{232}Th and ^{40}K in Bq/kg, respectively. The calculated absorbed dose rates were given in Table 1 and varied from 7.33 to 82.78 nGy h^{-1} with an average of 49.32 nGy h^{-1} which was lower than the world average value (57 nGy h^{-1}). The average dose rate for the world is 18–93 nGy h^{-1}, and a typical range for measured absorbed dose rates in outdoor air is 10–200 nGy h^{-1} [11]. The average contribution to the external radiation dose rate from natural radionuclides was as follows: 19.35% (9.62 nGy h^{-1}) for the U series, 42.05% (22.13 nGy h^{-1}) for the Th series, and 38.60% (17.57 nGy h^{-1}) for ^{40}K. With respect to worldwide median value determined by UNSCEAR report (31.72, 35.55, 32.73%, respectively), it could be observed that the contribution of Th series was higher, where that of U series was much lower [11].

As also listed in Table 2, except for the district of Kaiga in India, most of the values for the gamma ray dose rate from different area were relatively higher than that of this investigation due to the variations in the soil formation geology. However, the value in the present work was quite closed and comparable to that of previous study [7].

Calculation of outdoor annual effective dose (AED)

To estimate annual effective dose, the conversion coefficient and outdoor occupancy factor from absorbed dose in air must be considered to obtain the effective dose. In the UNSCEAR 1993 report [28], a conversion factor of 0.7 Sv Gy^{-1} and 0.2 by adults adopted as the outdoor occupancy factor were recommended to convert absorbed dose (nGy $^{-1}$) in air to annual effective dose which is determined by the following equation.

$$AED\,(\mu\mathrm{Sv\,a^{-1}}) = D\,(\mathrm{nGy\,h^{-1}}) \times 8760\,(\mathrm{h\,a^{-1}}) \times 0.7\mathrm{Sv\ Gy^{-1}} \times 0.2 \times 10^{-3} \quad (5)$$

As also shown in Table 1, the baseline average outdoor annual effective dose for the sampling sites to population was 60.48 μSv a^{-1}. About half of the sampling sites have values higher than the baseline average, whereas half of the locations have values below the baseline average. The baseline value for sites was lower than the recommended value of 70 μSv a^{-1}, which is the world average outdoor effective dose [29] for terrestrial habitants. For this recommended value, quite low probability of occurrence exists for either severe somatic or genetic health problems.

The effects of soil characteristics

On the basis of the physic-chemical analysis shown in Table 3 from the surveyed area, almost the soils comprised dominantly of sand, (clay + silt) with the order of magnitude being % (coarse + fine) sand > % (clay + silt). These soils could be classified as loamy sand and sand using USDA classification [30]. On the contrary, the sampling code 1 was classified as clay with lower activity concentration of ^{40}K (383 Bq/kg), which was also in accordance with the finding (382 Bq/kg) of previous

Table 4 Pearson correlations matrix among variables

	^{40}K	^{228}Ac	^{208}Tl	^{212}Bi	^{212}Pb	^{214}Bi	^{214}Pb	Density	pH	Conductivity	Coarse sand	Find sand	Clay + silt
^{40}K		0.675**	0.719**	0.680**	0.679**	0.572*	0.616*	−0.293	−0.542*	−0.523*	−0.376	0.338	0.245
^{228}Ac	0.004		0.986**	0.982**	0.987**	0.975**	0.982**	−0.418	−0.762**	−0.616*	0.035	−0.167	0.148
^{208}Tl	0.002	0.000		0.991**	0.988**	0.946**	0.954**	−0.493	−0.790**	−0.591*	0.019	−0.142	0.145
^{212}Bi	0.004	0.000	0.000		0.988**	0.951**	0.956**	−0.466	−0.797**	−0.571*	0.010	−0.133	0.151
^{212}Pb	0.004	0.000	0.000	0.000		0.953**	0.975**	−0.435	−0.829**	−0.576*	0.063	−0.159	0.088
^{214}Bi	0.021	0.000	0.000	0.000	0.000		0.982**	−0.390	−0.718**	−0.621*	0.107	−0.222	0.090
^{214}Pb	0.011	0.000	0.000	0.000	0.000	0.000		−0.413	−0.778**	−0.581*	0.084	−0.170	0.064
Density	0.270	0.107	0.053	0.069	0.092	0.135	0.112		0.300	−0.029	0.149	−0.195	−0.020
pH	0.030	0.001	0.000	0.000	0.000	0.002	0.000	0.258		0.534*	−0.193	0.211	0.079
Conductivity	0.038	0.011	0.016	0.021	0.020	0.010	0.018	0.915	0.033		0.154	0.094	−0.395
Coarse sand	0.151	0.896	0.943	0.971	0.816	0.694	0.756	0.581	0.474	0.568		−0.839**	−0.726**
Find sand	0.201	0.536	0.599	0.623	0.556	0.409	0.530	0.469	0.433	0.728	0.000		0.235
Clay + silt	0.361	0.584	0.591	0.578	0.746	0.741	0.815	0.940	0.772	0.130	0.001	0.380	

The right upper part is correlation coefficient; the left lower part is significant level

*Correlation is significant at the 0.05 level (two-tailed)

**Correlation is significant at the 0.01 level (two-tailed)

investigation in Taiwan [31]. The sample code 13, as white sand, collected from sea shore with the highest conductivity of 2510 μs/cm, might contain high salt contents. The salt content was normally measured in terms of electrical conductivity on an extract of the sand.

Correlation coefficient analysis results

With the objective of evaluating correlations between activity concentrations of radionuclides and the physico-chemical parameters, Pearson linear correlation coefficient test was used. The obtained correlation matrix was presented in Table 4. High correlations were observed between the natural radioisotopes of uranium series (^{214}Bi and ^{214}Pb) and thorium series (^{228}Ac, ^{212}Bi, ^{212}Pb and ^{208}Tl) with correlation coefficients more than 0.946 and this was in well agreement with the literature data [32]. ^{40}K had moderate correlation with uranium/thorium series members and weak correlation with pH and conductivity and no correlation with the distribution of soil size and density. No correlation between soil density and all natural radionuclides was also observed. Although the confidence level did not meet the criteria, $p < 0.05$, the correlation coefficient of fraction of clay and silt was higher 10 times than that of coarse sand for daughters of Th series. Natural radioactivity principally increased with the decrease of particle size similar to findings of other investigations [33, 34].

The soil characteristic, pH with extreme differences ranging from 3.93 and 8.23 (Table 3), exhibited significant or highly significant ($p < 0.01$) and negative correlation coefficients ($r = -0.829$ to -0.718) with uranium/thorium series members, suggesting that the transformation of the forms of radioactive elements was based on sorption interactions in combination with the migration of soil particles. The fixation of radionuclides was accompanied by the distribution of the elements between the main solid phase. Rachkova et al. [35] also stated that the precipitation of thorium hydrated oxide and the co-precipitation with iron hydroxides could play an important role in the processes of thorium removal from liquid phase in neutral and alkaline soils. In other words, the radionuclides extracted from a leached soil into the water in neutral and alkaline media could decrease and weaken the fixation of nuclides in the soil. The similar results of this study were consistent with the finding of literature [36] concerning about the effect of soil properties.

Cluster analysis

Cluster analysis (CA) is one of multivariate techniques used to identify and classify groups with similar characters in a new group of observations. Each observation in a

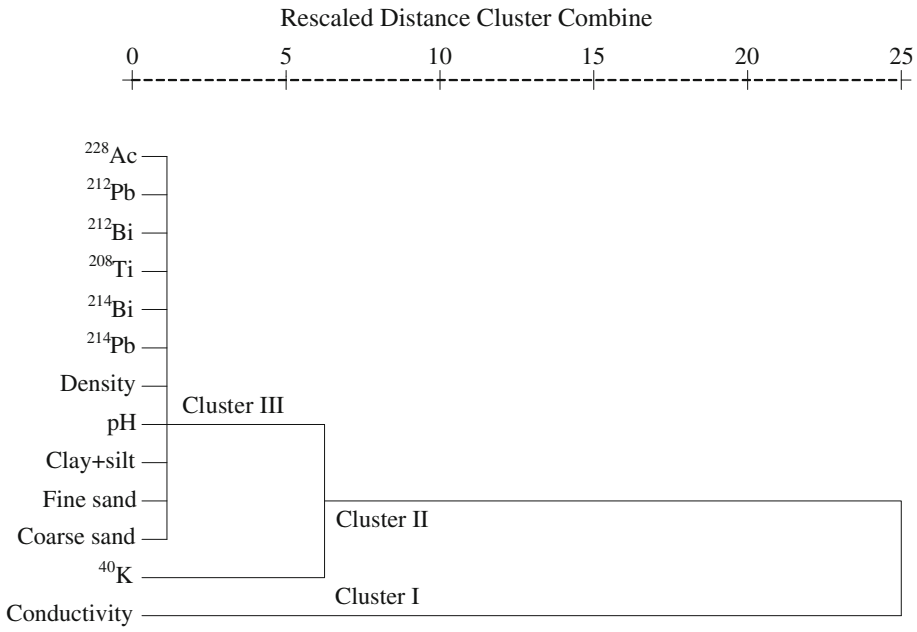

Fig. 2 Dendrogram using average linkage of hierarchical cluster analysis for 13 variables

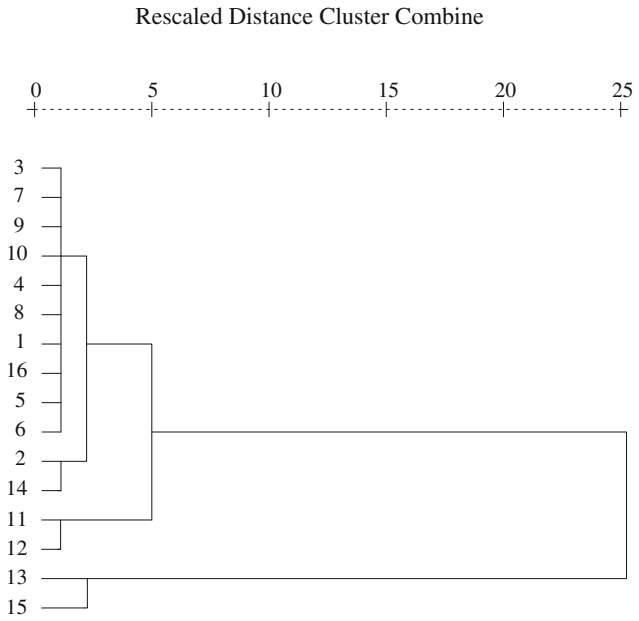

Fig. 3 Dendrogram (Euclidean distances) based on the soil parameters at all sampling stations

Table 5 Rotated component matrix for data of soil

Variable	PC1	PC2	PC3	Communalities
K-40	**0.70**	**0.47**	−0.06	0.71
Ac-228	**0.99**	0.01	0.00	0.98
Tl-208	**0.99**	0.04	−0.07	0.99
Bi-212	**0.98**	0.04	−0.06	0.97
Pb-212	**0.99**	−0.02	−0.06	0.98
Bi-214	**0.96**	−0.07	0.02	0.93
Pb-214	**0.97**	−0.05	−0.04	0.95
Density	**−0.43**	−0.18	**0.72**	0.75
pH	**−0.83**	0.16	0.02	0.72
Conductivity	**−0.65**	−0.21	**−0.58**	0.81
Coarse sand	0.05	**−0.99**	0.00	0.99
Find sand	−0.17	**0.83**	−0.37	0.85
Clay + silt	0.12	0.72	**0.46**	0.75
Eigenvalue	7.63	2.52	1.22	
% of variance explained	58.7	19.4	9.4	
% of cumulative	58.7	78.1	87.5	

PCA loadings > 0.4 or < 0.4 were shown in bold

Extraction method: principal component analysis. Rotation method: varimax with Kaiser normalization. Rotation converged in three iterations

cluster is most like others in the same cluster. Similarity is a measure of distance between clusters relative to the largest distance between any two individual variables. The zero distance means the clusters are 100% similarity in their sample measurements, whereas the cluster areas are as disparate as the least similar region means similarity of 0%. Cluster analysis was carried out through two axes; the first was to identify sampling locations with similar characters. The other axis was to identify similar characteristics among natural radioisotopes and parameters in the soil.

In CA, the average linkage method along with correlation coefficient distance was applied and the derived dendrogram was shown in Fig. 2. In this dendrogram, all 13 parameters were grouped into three statistically significant clusters. Cluster I was conductivity; cluster II was ^{40}K and cluster III consisted of natural radionuclides, density, pH and soil size distribution, which appeared in the same cluster. All of the natural radioisotopes were represented as one group with similar characteristics as they originated

from ^{232}Th and ^{238}U series. ^{228}Ac, ^{212}Pb ^{212}Bi, and ^{208}Tl were close to each other. Likewise, ^{214}Bi and ^{214}Pb were close to each other. ^{40}K was identified in another group order far from the other radioisotopes and grouped closely with the group of grain size distribution. The close relation between ^{238}U and ^{232}Th series members but not with ^{40}K was in accordance with the results [31, 37].

Figure 3 showed dendrogram of classification of the sampling locations as groups according to the soil parameters. In this dendrogram, cluster analysis has been classified sampling no, 13 and 15 as more unique locations ascribed to the lower activity concentrations of ^{238}U and ^{232}Th series with much higher conductivity and pH value and the presence of coast white sand and sedimentary sand, respectively. The sampling stations, 11 and 12 collected from the river sand around nuclear power plants of Chin-San and Shih-Men, respectively were grouped into one cluster due to relatively close activity concentrations of ^{238}U and ^{232}Th series, pH value and conductivity. The sampling codes in their characters from 3, 7, 9, 10, 4, 8, 1, 16, 5 and 6 were grouped as much closed locations in a big group.

Principal component analysis

Principal component analysis (PCA) was applied to identify variables by applying varimax rotation with Kaiser Normalization. By extracting the eigenvalues and eigenvectors from the correlation matrix, the number of significant factors and the percent of variance explained by each of them were calculated. Table 5 displayed the results of the factor loadings with a varimax rotation, as well as the eigenvalues and communalities. The results showed that there were three eigenvalues higher than one and that these three factors could explain over 87% of the total variance. Normally, an ordination result was good if the value was 75% or better [38]. The first component (PC1) explained 58.7% of the total variance and loaded heavily on uranium and thorium series. The second component (PC2), was correlated very strongly with coarse sand and fine sand with a high loading value (−0.99 and 0.83, respectively), accounting for 19.4% of the total variance. The third component (PC3) was loaded primarily by density and also moderately by conductivity and clay + silt, accounting for 9.4% of the total variance.

Conclusions

Analytical results demonstrated that no radiological anomaly was found for the survey. The following is a list of major findings.

1. Activity concentrations of ^{238}U, ^{232}Th and ^{40}K sampling locations were within the world range and the gamma absorbed dose rates and annual effective dose of were within world median ranges.
2. The calculated values of hazard indices were lower than unity while the soil could be used as building material, indicating that samples were not a significant source of radiation hazard. From a radiological point of view, the studied area in Taiwan was safe for the population as a consequence of terrestrial gamma radiation.
3. No correlation between soil density and all natural radionuclides was also observed. However, a significant and negative relationship was observed between natural radionuclide contents and pH values in the soil samples based on analytical results of Pearson correlation coefficient.
4. The quite close relation for natural radionuclides of the U and Th series, soil density, pH value and grain size distribution was clustered as one group, whereas the conductivity was recognized in another group far from the other soil parameters and radioisotopes. ^{40}K was recognized in one separate group and had obvious differences with other radioisotopes.
5. The sampling codes of 13 (NPP3 coast white sand) and 15 (NPP1 sedimentary sand) were classified more unique locations resulting from the lower activity concentrations of U and Th series, much higher conductivity and pH value.
6. The principal component analysis explained 87.5% of the data variability through three factors. Therefore, instead of 13 soil parameters, three combined variables provided the basic variation information about the data.

Acknowledgments The authors would like to thank Mr. Lo of Radiation Monitoring Center of Atomic Energy Council for the measurement and useful advice in using gamma spectrometer. The authors would like to express their grateful appreciation to Mr. Ching-Her Yang and Mr. Ho-Chuan Huang for their technical assistance. Dr. Gia-Luen Guo, a researcher working on the Cellulosic Ethanol Project at Institute of Nuclear Energy Research (INER) is also acknowledged for providing valuable information and generous support in cartography of the geological map during this work.

References

1. Chu TC, Weng PS, Lin YM (1992) Distribution of naturally occurring radionuclides in Taiwanese rocks. Radiat Prot Dosim 45(1/4):281–283
2. The Geology of Taiwan. http://twgeog.geo.ntnu.edu.tw/english/geology/geology.htm#
3. Tzortzis M, Svoukis E, Tsertos H (2004) A comprehensive study of natural gamma radioactivity levels and associated dose rates from surface soils in Cyprus. Radiat Prot Dosim 109:217–224
4. El-Arabi AM (2005) Natural radioactivity in sand used in thermal therapy at the Red Sea Coast. J Environ Radioact 81:11–19

5. Karakelle B, Öztűrk N, Köse A, Varinlioğlu A, Erkol AY, Yilmaz F (2002) Natural radioactivity in soil samples of Kocaeli basin, Turkey. J Radioanal Nucl Chem 254:649–651
6. Geology of NORM (2004) http://www.tenorm.com/geo.htm. Accessed 6 Sep 2004
7. Tsai TL, Lin CC, Wang TW, Chu TC (2008) Radioactivity concentrations and dose assessment for soil samples around nuclear power plant IV in Taiwan. J Radiol Prot 28:347–360
8. Patra AK, Sudhakar J, Ravi PM, James JP, Hegde AG, Joshi ML (2006) Natural radioactivity distribution in geological matrices around Kaiga environment. J Radioanal Nucl Chem 270(2): 307–312
9. Facchinelli A, Sacchi E, Mallen L (2001) Multivariate statistical GIS-based approach to identify heavy metal sources in soils. Environ Pollut 114:313–324
10. Ramasamy V, Suresh G, Meenakshisundaram V, Ponnusamy V (2011) Horizontal and vertical characterization of radionuclides and minerals in river sediments. Appl Radiat Isot 69:184–195
11. UNSCEAR (2000) Sources, effects and risks of ionization radiation. Report to the general assembly, with scientific annexes B: Exposures from natural radiation sources. UNSCEAR New York
12. Jabbar T, Subhani MS, Khan K, Rashid A, Orfi SD, Khan AY (2003) Natural and fallout radionuclide concentrations in the environment of Islamabad. J Radioanal Nucl Chem 258(1): 143–149
13. Quindós LS, Fernández PL, Soto J, Ródenas C, Gómez J (1994) Natural radioactivity in Spanish soils. Health Phys 66(2):194–200
14. Ibrahim NM, Abd El Ghani AH, Shawky EM, Ashraf EM, Farouk MA (1993) Measurement of radioactivity levels in soils in the Nile Delta and Middle Egypt. Health Phys 64:620–627
15. Miah FK, Roy S, Touchiduzzaman M, Alam B (1998) Distribution of radionuclides in soil samples in and around Dhaka city. Appl Radiat Isot 49:133–137
16. Yu KN, Guan ZJ, Stokes MJ, Young ECM (1992) The assessment of the natural radiation dose committed to the Hong Kong people. J Environ Radioact 17(1):31–48
17. Chen CJ, Weng PS, Chu TC (1993) Evaluation of natural radiation in houses built with black schist. Health Phys 64(1):74–78
18. Selvasekarapandian S, Manikandan NM, Sivakumar R, Meenakshisundaram V, Raghunath VM (2002) Natural radiation distribution of soils at Kotagiri Taluk of the Nilgiris biosphere in India. J Radioanal Nucl Chem 252(2):429–435
19. Ereeş FS, Akőzcan S, Parlak Y, Çam S (2006) Assessment of dose rates around Manisa (Turkey). Radiat Meas 41:598–601
20. Jabbar A, Arshed W, Bhatti AS, Ahmad SS, Saeed-Ur-Rehman DilbandM (2010) Measurement of soil radioactivity levels and radiation hazard assessment in mid Rechna interfluvial region, Pakistan. J Radioanal Nucl Chem 283(2):371–378
21. La Breque JJ (1994) Distribution of ^{137}Cs, ^{40}K, ^{238}U and ^{232}Th in soils from northern Venezuela. J Radioanal Nucl Chem 178(2): 327–336
22. Örgün Y, Altınsoy N, Şahin SY, Güngőr Y, Gültekin AH, Karaham G, Karacık Z (2007) Natural and anthropogenic radionuclides in rocks and beach sands from Ezine region (Çanakkale), Western Anatolia, Turkey. Appl Radiat Isot 65:739–747
23. Yasir MS, Majid AAb, Yahaya R (2007) Study of natural radionuclides and its radiation hazard index in Malaysian building materials. J Radioanal Nucl Chem 273(3):539–541
24. Beretka J, Matthew PJ (1985) Natural radioactivity of Australian building materials, industrial waste, and by-products. Health Phys 48:87–95
25. Krieger R (1981) Radioactivity of construction materials. Betonwerk Fertigteil Techn 47:468–473
26. Commission European (1999) Radiation protection 112 radiological protection principles concerning the natural radioactivity of building materials. European Commission, Brussels
27. Beck HL, Decompo J, Gologak J (1972) In situ Ge (Li) and NaI (Tl) gamma-ray spectrometry Report 258. Health and Safety Laboratory, US Atomic Energy Commission
28. UNSCEAR (1993) sources and effects of ionization radiation. Report to the general assembly, with scientific annexes A: Exposures from natural radiation sources. UNSCEAR New York
29. UNSCEAR (1998) sources and effects of ionization radiation. Report to the general assembly, with scientific annexes B: Exposures from natural radiation sources. UNSCEAR New York
30. Miller S (1994) Handbook of agrohydrology. Natural Resources Institute, Chatham
31. Chen CJ, Huang CC, Yeh CH (2001) Introduction to natural background radiation in Taiwan. Phys Bimonthly 23(3):441–443
32. Nasr S, El-Gamal A, Hendawi I, Naim M (2006) Statistical evaluation of natural radioactivity in sediments along the Egyptian Mediterranean coast. In:Proceedings of the 2nd environmental physics conference, Alexandria, Egypt, 18–22 Feb 2006
33. Shetty PK, Narayana Y, Siddappa K (2006) Vertical profiles and enrichment pattern of natural radionuclides in monazite areas of coastal Kerala. J Environ Radioact 86:32–142
34. Belivermis M, Kılıç Ö, Çotuk Y, Topcuoğlu S (2010) The effects of physico-chemical properties on gamma emitting natural radionuclide levels. Environ Monit Assess 163:15–26
35. Rachkova NG, Shuktomova II, Taskaev AI (2010) The state of natural radionuclides of uranium, radium, and thorium in soils. Eurasian Soil Sci 43(6):651–658
36. Skarlou V, Papanciolaou EP, Nobeli C (1996) Soil to plant transfer of radioactive cesium and its relation to soil and plant properties. Geoderma 72:53–63
37. Elejalde C, Herranz M, Romero F, Legarda E (1996) Correlations between soil parameters and radionuclide contents in samples from Biscay (Spain). Water Air Soil Pollut 89:23–31
38. Zhang H, Lu YL, Dawson RW, Dawson ShiYJ, Wang TY (2005) Classification and ordination of DDT and HCH in soil samples from the Guanting Reservoir, China. Chemosphere 60:762–769